# Advanced Flicker Spectroscopy of Fluid Membranes

Hans-Günther Döbereiner,[1,*] Gerhard Gompper,[2] Christopher K. Haluska,[1] Daniel M. Kroll,[3] Peter G. Petrov,[1,†] and Karin A. Riske[1]

[1]*Max-Planck-Institut für Kolloid- und Grenzflächenforschung, Am Mühlenberg 1, 14476 Golm, Germany*
[2]*Institut für Festkörperforschung, Forschungszentrum Jülich, 52425 Jülich, Germany*
[3]*Department of Medicinal Chemistry and Minnesota Supercomputer Institute, University of Minnesota, 308 Harvard Street SE, Minneapolis, Minnesota 55455, USA*

(Received 26 June 2002; published 23 July 2003)

The bending elasticity of a fluid membrane is characterized by its modulus and spontaneous curvature. We present a new method, advanced flicker spectroscopy of giant nonspherical vesicles, which makes it possible to simultaneously measure both parameters for the first time. Our analysis is based on the generation of a large set of reference data from Monte Carlo simulations of randomly triangulated surfaces. As an example of the potential of the procedure, we monitor thermal trajectories of vesicle shapes and discuss the elastic response of zwitterionic membranes to transmembrane *p*H gradients. Our technique makes it possible to easily characterize membrane curvature as a function of environmental conditions.

DOI: 10.1103/PhysRevLett.91.048301 PACS numbers: 82.70.Uv, 05.40.–a, 87.16.Dg

The bending elasticity of amphiphilic interfaces is a fundamental concept introduced more than 30 years ago by Helfrich [1] to describe the morphology of biomembranes. Subsequently, it has been extensively applied to model the elastic behavior of soft interfaces [2–4]. The principal parameters characterizing the elastic energy of an amphiphilic interface are the bending modulus $\kappa$, which sets the energy scale, and the effective spontaneous curvature $\bar{C}_0$, which describes the preferred curvature of the interface. In this Letter we describe a new procedure which makes it possible, for the first time, to *simultaneously* determine both the bending modulus and the spontaneous curvature of a membrane in a single experiment.

There exist several techniques for measuring the bending modulus [5–7]. The method most widely used for membranes of higher bending rigidity is the flicker spectroscopy of giant, quasispherical vesicles [5,7]. Although this technique can be used to determine precise values of $\kappa$, it has the disadvantage that analytical results required for extracting $\kappa$ from experimental data are only available in the spherical limit. In this limit, the membrane is under a lateral tension which dominates the long-wavelength part of the spectrum. To determine $\kappa$ it is therefore necessary to measure the spectrum up to high mode number, which in turn requires very large vesicles. In addition, since the volume-to-area ratio changes with temperature, a vesicle which is quasispherical at one temperature is not quasispherical at another, so that the bending modulus of a single vesicle cannot be determined as a function of temperature. Finally, membrane fluctuations are insensitive to the effective spontaneous curvature in this limit, so that $\bar{C}_0$ cannot be determined.

Although values for the spontaneous curvature of various lipid molecules forming an inverted hexagonal phase [8] have been inferred, there is little experimental literature dealing with bilayer spontaneous curvature [9,10]. This is somewhat surprising since spontaneous curvature plays the key role in determining the morphology of biomembranes [2], lipid vesicles [3], and polymersomes [11]. Spontaneous curvature is crucial for maintaining the spatial organization of, and traffic between, cellular organelles and the plasma membrane; e.g., there is growing evidence for a coupling between cell signaling and endocytosis [12]. Further, the functional state of certain integral membrane proteins [13,14] and membrane fusion competence [15] is thought to be controlled by monolayer spontaneous curvature. More generally, control of interfacial curvature is required to tune the structure of materials on the nanoscale [16]. It is therefore important to develop a simple, straightforward procedure for the direct determination of the spontaneous curvature and bending modulus. The technique we have developed — flicker spectroscopy of nonspherical vesicles — avoids the shortcomings of traditional spectroscopy techniques by utilizing extensive Monte Carlo simulations of dynamically triangulated vesicles to generate data for a wide range of reduced volumes and spontaneous curvatures, which can then be used to extract the elastic parameters of the membrane from flicker spectroscopy data (see Fig. 1).

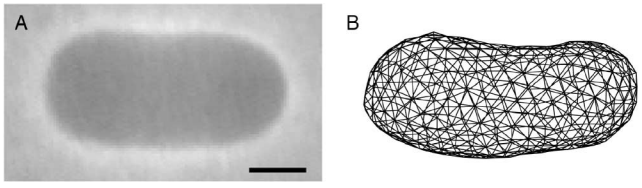


FIG. 1. Experimental and theoretical vesicle shapes. (A) Phase contrast micrograph ($v = 0.828$). The scale bar corresponds to 5 $\mu$m, (B) simulation snapshot. The parameters in the simulations are $v = 0.825$, $\kappa/k_BT = 25$, $\alpha = 0.90$, $\bar{c}_0 = -0.28$, and $g = 0.37$.

  

The fluctuation spectra contain information on both the bending modulus and the spontaneous curvature. Using this technique it is therefore possible to determine *both* elastic constants simultaneously from one experiment and to study their dependence on environmental conditions, such as temperature and solvent *p*H.

Experimentally, thermal shape fluctuations of giant fluid vesicles are well characterized using light microscopy [5,10,17]. In these experiments, fluctuating prolate vesicles are stabilized by gravity — due to a small density difference of the solvent inside and outside the vesicle — on the bottom of a temperature-controlled microchamber. The focal plane of a phase contrast microscope is adjusted to include the long axis of the vesicle, and shape contours are obtained by real time video image analysis; for details see Ref. [17]. The raw data therefore consist of a time sequence of closed 2D loops. Choosing a coordinate system in which the $x$ coordinate lies along the long axis of the vesicle, the contours are then represented in polar coordinates $(r, \varphi)$ as $r(\varphi) = r_0[1 + \sum_n a_n \cos(n\varphi) + \sum_n b_n \sin(n\varphi)]$, where the angle $\varphi$ is measured from the positive $x$ axis. The time-dependent amplitudes $\{a_n, b_n\}$ encode the full experimental information. The mean values $\langle a_n \rangle$ describe the mean vesicle shape; for the oriented contours used here, $\langle b_n \rangle = 0$. The mean-square amplitudes $\langle \Delta a_n^2 \rangle \equiv \langle (a_n - \langle a_n \rangle)^2 \rangle$ measure the thermal fluctuations of the vesicles about their mean shape.

Our Monte Carlo simulations are based on a model of dynamically triangulated surfaces [18]. The bilayer membrane is modeled by a single triangulated network of spherical topology; see Fig. 1(B). In contrast to previous simulations [19], we use the full Hamiltonian of the area-difference-elasticity model [20] and include the contribution of a gravitational force acting on the vesicle interior [21]. The discretization of the mean curvature is described in Ref. [18]. The ratio of volume $V$ and area $A$ of the vesicles is characterized by the reduced volume $v = (R_V/R_A)^3$, where $R_A = (A/4\pi)^{1/2}$ and $R_V = (3V/4\pi)^{1/3}$ are effective vesicle radii. The influence of gravity is measured via the dimensionless parameter $g = g_0 \Delta\rho R_A^4/\kappa$, where $g_0$ is the local acceleration and $\Delta\rho$ is the excess mass density of the interior vesicle solution.

The membrane asymmetry is measured by the dimensionless parameter $\bar{c}_0 = \bar{C}_0 R_A$. The effective spontaneous curvature $\bar{C}_0$ has two contributions [17]: the first is due to solution and/or bilayer asymmetry, the second — which is weighted by the ratio $\alpha$ of the membrane stretching modulus to the bending rigidity ($\alpha \simeq 1.4$ for phosphocholine bilayers [20]) — is due to the area difference in the inner and outer monolayers. These two contributions cannot be independently determined from a single vesicle fluctuation spectrum [17].

The Monte Carlo simulations follow the procedure described previously [18]. In order to extract the experimentally relevant information, we first fit the simulated three-dimensional shape data using an expansion in spherical harmonics. The Fourier expansion of the two-dimensional contour in a plane through the center of mass, parallel to the substrate, is easily obtained from this fit. Most of our data are obtained for triangulated surfaces of 407 vertices; the shapes are fitted with 196 spherical harmonics, which implies some smoothing of the simulated shapes on the scale of the lattice constant. The simulated vesicles are therefore analyzed in the same way as real vesicles in experiment. We characterize the mean vesicle shape by the first two amplitudes $\langle a_2 \rangle$ and $\langle a_4 \rangle$, which is known to be a very good approximation [17]. With increasing $\bar{c}_0$, a transition from an oblate to a prolate shape is observed, which leads to a pronounced increase of $\langle a_2 \rangle$ and $\langle a_4 \rangle$. The oblate-to-prolate transition is reflected in a sharp peak of the fluctuations in $a_2$; see Fig. 2. Similarly, the budding transition of the prolate shapes, which occurs at higher spontaneous curvature, is signaled by a strong increase of the mean-square amplitude $\langle \Delta a_3^2 \rangle$ as the budding spinodal is approached (data not shown).

The fitting of the experimental spectra to the Monte Carlo data sets proceeds as follows. We employ the average amplitudes $\langle a_2 \rangle$, $\langle a_4 \rangle$, and the mean-square fluctuation amplitudes $\langle \Delta a_2^2 \rangle$, $\langle \Delta a_3^2 \rangle$, $\langle \Delta a_4^2 \rangle$, and $\langle \Delta a_5^2 \rangle$. The Monte Carlo data of all these quantities are first interpolated linearly as a function of $\bar{c}_0$, then again linearly as a function of the reduced volume $v$. A least-square fit to the experimental data then determines $\kappa$, $\bar{c}_0$, and $v$ simultaneously for a given vesicle.

The analysis of 14 prolate stearoyl-oleoyl-phosphatidylcholine (SOPC) vesicles in sucrose/glucose solution (100 mM) yielded results for the bending modulus which clustered around two values, $\kappa = (35 \pm 3) k_B T$ and $\kappa = (75 \pm 7) k_B T$, corresponding to single and double

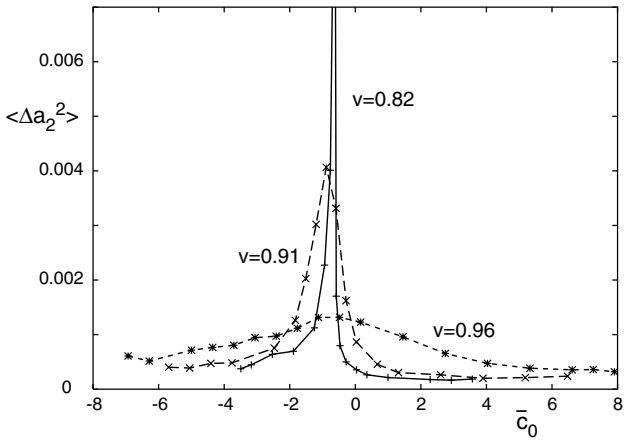


FIG. 2. Simulated mean-square amplitude $\langle \Delta a_2^2 \rangle$ of shape fluctuations as a function of the effective spontaneous curvature $\bar{c}_0$. Note the peak at the prolate-to-oblate transition. Three different values of the reduced volume are shown, as indicated. The other parameters are $\kappa/k_B T = 25$, $\alpha = 0.90$, and $g = 0.37$.

bilayer membranes, respectively. The measured bending modulus is in good agreement with the value $\kappa = 32k_BT$ obtained from fluctuation spectroscopy of quasispherical vesicles [7]. It is important to point out that we can analyze vesicles as small as 3–4 $\mu$m, which is much smaller than those used in Ref. [7].

In order to test our ability to determine the spontaneous curvature, we explored thermal shape trajectories of SOPC vesicles in parameter space $(v, \bar{c}_0)(T)$. A suitable vesicle was selected and driven via temperature across two shape transitions. We followed the vesicle from an oblate shape at low temperatures ($T < 23.0\,^\circ$C), through an elongated prolate form at higher temperatures, to the budding transition ($T = 44.0\,^\circ$C). We obtain $\kappa = (35 \pm 5)k_BT$ for the mean bending modulus. The reduced volume $v$ and spontaneous curvature $\bar{c}_0$ both vary approximately linearly with temperature. In the prolate phase, we obtain a thermal expansion coefficient $\beta_A = (1.9 \pm 0.1) \times 10^{-3}/K$, consistent with the results of Ref. [22]. In Fig. 3, the mapped $(\bar{c}_0, v)$ trajectory is shown together with the two ($T = 0$) spinodal lines of the prolate phase. Linear extrapolation to obtain the crossing points with the two spinodals gives $v^s_{\text{bud}} = 0.777$ and $v^s_{\text{pro/obl}} = 0.830$. Comparison with the reduced volumes, where budding ($v_{\text{bud}} = 0.775$) and the prolate-oblate transition ($v_{\text{pro/obl}} = 0.834$) actually occurred, shows a nice agreement. These results clearly demonstrate that we are able to extract precise values for the elastic parameters of the membrane using our technique.

We have also employed the method to measure electrostatically induced spontaneous curvature. It has been suggested that a change in $p$H induces membrane curvature via association of hydroxyl ions with the trimethylammonium group of the phosphatidylcholine molecule [23]. In order to quantify such an effect, we have swollen giant SOPC vesicles in raffinose solution at neutral $p$H and incubated them in an equiosmolar solution of glucose and 50 $\mu$M potassium hexacyanoferrate, which is therefore present only on the outside of the vesicle. Illuminating the sample leads to an increase of $p$H in the external solution due to photoaquation of the iron complex, as well as a subsequent curvature change of the vesicle membrane [24]. The magnitude of the $p$H change depends on the illumination intensity. We have calibrated the $p$H change in the external vesicle solution using the fluorescent probe 4-methylumbelliferone.

Figure 4 contains normalized histograms of the elliptical mode $a_2$ of a typical vesicle as a function of external $p$H. At low $p$H, the vesicle is in a bistable state with a predominantly oblate shape. It shows pronounced prolate-oblate fluctuations due to the proximity of the weak first-order prolate-oblate transition. At elevated $p$H values, the prolate shape is stable. Note the strong fluctuations even at this $p$H. Two effects are visible. First, the vesicle contour becomes more elliptical with increasing $p$H. Second, the fluctuations in the elliptical mode decrease. As we have seen above (compare Fig. 2), the latter indicates that the prolate vesicle is moving away from the prolate-oblate transition; i.e., the spontaneous curvature increases. The apparent elongation of the vesicle is due to competition between bending elastic energy and gravity. The vesicle becomes progressively less flattened by gravity with increasing spontaneous curvature. This tends to drive the vesicle towards the budding transition, where a small satellite is expelled along the polar axis. Indeed, at sufficiently high $p$H we observed, in general, budding of the vesicle, signaled by an increase in pearlike vesicle fluctuations near the budding instability. For the vesicle shown in Fig. 4, we found $\langle \Delta a_3^2 \rangle = 0.0204$ ($p$H 7.7), 0.0267 ($p$H 8.1), and 0.0288 ($p$H 8.5).

The results of the fitting procedure described above are shown in Fig. 5. As already anticipated from the raw data,

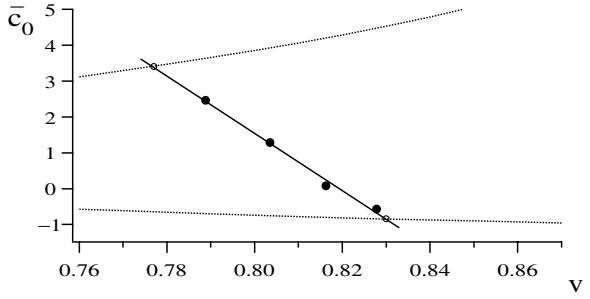


FIG. 3. Thermal trajectory of a prolate vesicle in $(\bar{c}_0, v)$ parameter space with a radius $R_A = 4.8$ $\mu$m and $g = 0.21$. The experimental points correspond to temperatures $T = 25.0\,^\circ$C, $29.4\,^\circ$C, $34.2\,^\circ$C, and $38.8\,^\circ$C. The crossing points of a linear fit to the trajectory with the upper (budding) and lower spinodal (prolate-oblate transition) are indicated. For the bending modulus we find $\kappa = (35 \pm 5)k_BT$.

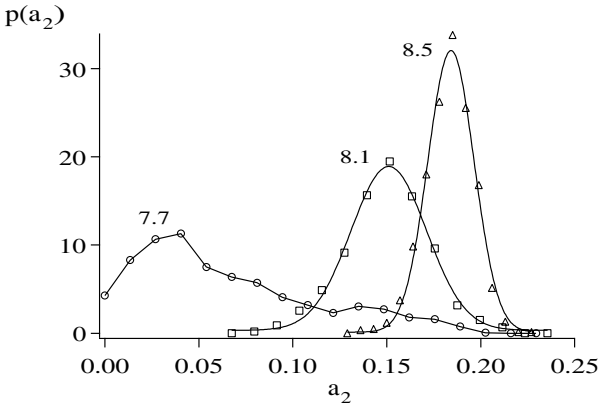


FIG. 4. Normalized histograms [$\int p(a)da = 1$] of the elliptical shape fluctuations of a prolate SOPC vesicle ($R_A = 5.2$ $\mu$m) with varying external $p$H of 7.7 (open circles), 8.1 (open squares), and 8.5 (open triangles) at constant internal $p$H 7.7. Gaussian fits are shown. With increasing $p$H gradient the vesicle develops a more elongated shape (larger $a_2$) with decreasing fluctuations.

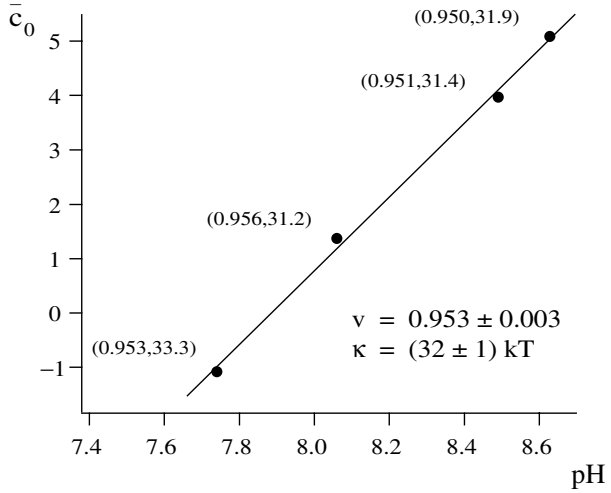


FIG. 5. Spontaneous curvature $\bar{c}_0$ as a function of external $p$H for $g = 0.8$. Note that the reduced volume and bending modulus, which are given in brackets, $(v, \kappa)$, remain constant. $v$, $c_0$, and $\kappa$ are obtained simultaneously via comparison of the data shown in Fig. 4 to Monte Carlo simulations.

we find a strong change in spontaneous curvature at a constant bending modulus $\kappa = (32 \pm 1)k_BT$. Indeed, the bending modulus of SOPC (see the measurement above) should not change considerably since electrostatic contributions to the elastic modulus are only on the order of $1k_BT$ [25]. Note that the reduced volume of the vesicle, $v = 0.953 \pm 0.003$, is also found to be constant, as it should be. This is a nontrivial result of the fit considering the large changes in apparent area of the vesicle with $p$H. The large increase in the spontaneous curvature can be understood by considering the balance of the electrostatic free energy and the intrinsic bending energy of the membrane.

In summary, we have developed a general technique which makes it possible to determine simultaneously both the bending modulus and the spontaneous curvature of a fluid membrane. The general idea is to use a single nonspherical vesicle as a morphological probe of the (elastic) interactions of its membrane with the surrounding fluid. A large number of phenomena can be monitored by analysis of the vesicle fluctuation spectrum. In addition to characterizing the static curvature response to environmental conditions, the dynamics of (bio-)chemical reactions at interfaces can be monitored. This has important consequences for future studies dealing with biological or material aspects of interfacial elasticity.

H. G. D. wants to thank U. Seifert and W. Fenzl for enjoyable and helpful discussions. H. G. D. is grateful to R. Lipowsky for the opportunity to do this work at his department and thanks him and the Deutsche Forschungsgemeinschaft for financial support. D. M. K. acknowledges support from the National Science Foundation under Grant No. DMR-0083219, and the donors of The Petroleum Research Fund, administered by the ACS.

*Present address: Department of Biological Sciences, Columbia University, New York, NY 10027.
†Permanent address: School of Physics, University of Exeter, EX4 4QL, United Kingdom.

[1] W. Helfrich, Z. Naturforsch. **28c**, 693 (1973).
[2] *Handbook of Biological Physics*, edited by R. Lipowsky and E. Sackmann (Elsevier, Amsterdam, 1995), Vol. I.
[3] U. Seifert, Adv. Phys. **46**, 13 (1997).
[4] S. A. Safran, Adv. Phys. **48**, 395 (1999).
[5] H. P. Duwe, J. Käs, and E. Sackmann, J. Phys. I (France) **51**, 945 (1990).
[6] E. Evans and W. Rawicz, Phys. Rev. Lett. **64**, 2094 (1990).
[7] P. Méléard, C. Gerbeaud, T. Pott, L. Fernandez-Puente, I. Bivas, M. D. Mitov, J. Dufourcq, and P. Bothorel, Biophys. J. **72**, 2616 (1997).
[8] N. Fuller and R. P. Rand, Biophys. J. **81**, 243 (2001), and references therein.
[9] W. Harbich, H. J. Deuling, and W. Helfrich, J. Phys. (Paris) **38**, 727 (1977).
[10] H.-G. Döbereiner, O. Selchow, and R. Lipowsky, Eur. Biophys. J. **28**, 174 (1999).
[11] B. M. Discher, Y.-Y. Won, D. S. Ege, J. C-M. Lee, F. S. Bates, D. E. Discher, and D. A. Hammer, Science **284**, 1143 (1999).
[12] A. Petrelli, G. F. Gilestro, S. Lanzardo, P. M. Comoglio, N. Migone, and S. Giordano, Nature (London) **416**, 187 (2002).
[13] S. L. Keller, S. M. Bezrukov, S. M. Gruner, M. W. Tate, I. Vodyanoy, and V. A. Parsegian, Biophys. J. **65**, 23 (1993).
[14] G. S. Attard, R. H. Templer, W. S. Smith, A. N. Hunt, and S. Jackowski, Proc. Natl. Acad. Sci. U.S.A. **97**, 9032 (2000).
[15] B. R. Lentz, D. P. Siegel, and V. Malinin, Biophys. J. **82**, 555 (2002).
[16] R. Strey, Colloid Polym. Sci. **272**, 1005 (1994).
[17] H.-G. Döbereiner, E. Evans, M. Kraus, U. Seifert, and M. Wortis, Phys. Rev. E **55**, 4458 (1997).
[18] G. Gompper and D. M. Kroll, J. Phys. Condens. Matter **9**, 8795 (1997).
[19] G. Gompper and D. M. Kroll, Phys. Rev. Lett. **73**, 2139 (1994).
[20] L. Miao, U. Seifert, M. Wortis, and H.-G. Döbereiner, Phys. Rev. E **49**, 5389 (1994).
[21] M. Kraus, U. Seifert, and R. Lipowsky, Europhys. Lett. **32**, 431 (1995).
[22] D. Needham, T. J. McIntosh, and E. Evans, Biochemistry **27**, 4668 (1988).
[23] J. B. Lee, P. G. Petrov, and H.-G. Döbereiner, Langmuir **15**, 8543 (1999).
[24] P. G. Petrov, J. Lee, and H.-G. Döbereiner, Europhys. Lett. **48**, 435 (1999).
[25] T. Chou, M. V. Jaric, and E. D. Siggia, Biophys. J. **72**, 2042 (1997).